

Sugarcane Water Productivity Assessments in the São Paulo state, Brazil

Antônio H. de C. Teixeira^{*1}, Janice F. Leivas², Carlos C. Ronquim³, Daniel de C. Victoria⁴

^{1,2,3}Embrapa Satellite Monitoring; ⁴Embrapa Agriculture Informatics Campinas, São Paulo, Brazil

^{*1}heriberto.teixeira@embrapa.br; ²janice.leivas@embrapa.br; ³carlos.ronquim@embrapa.br;

⁴daniel.victoria@embrapa.br

Abstract

São Paulo state, Brazil, has been highlighted by the sugarcane crop expansion. The actual scenario of climate and land use changes, bring attention for the large-scale water productivity (WP) analyses. MODIS images were used together with gridded weather data for these analyses. A generalized sugarcane growing cycle inside a crop land mask, from September 2011 to October 2012, was considered in the main growing regions of the state. Actual evapotranspiration (ET) is quantified by the SAFER (Simple Algorithm for Evapotranspiration Retrieving) algorithm, the biomass production (BIO) by the RUE (Radiation Use Efficiency) Monteith's model and WP is considered as the ratio of BIO to ET. During the four generalized sugarcane crop phases, the mean ET values ranged from 0.6 to 4.0 mm day⁻¹; BIO rates were between 20 and 200 kg ha⁻¹ day⁻¹, resulting in WP ranging from 2.8 to 6.0 kg m⁻³. Soil moisture indicators are applied, indicating benefits from supplementary irrigation during the grand growth phase, wherever there is water availability for this practice. The quantification of the large-scale water variables may subsidize the rational water resources management under the sugarcane expansion and water scarcity scenarios.

Keywords

Remote Sensing; Evapotranspiration; Biomass Production; Water Resources; Bioenergy Crop

Introduction

In Brazil, sugarcane (*Saccharum officinarum*) crop has increased, for both sugar and alcohol production, but also with the perspective of generating renewable energy [1]. In the São Paulo state, besides climate alterations, land use changes have been taking place, because of the expansion of these activities in several regions with climatic aptitude.

The negative effects, in areas before occupied by natural vegetation, citrus, grains, and coffee [2] could be more harmful when comparing with those from the fossil fuel exploration, regarding greenhouse gas emissions [3].

On one hand, aiming bioenergy production, a crop should be fast growing and high yielding with its energy output exceeding fossil fuel energy input. In terms of satisfying these criteria, sugarcane is currently the most promising energy crop [4]. On the other hand, its cultivation increases regional water demands [5] and there are many concerns about the impacts on the carbon cycle [6]; further affecting the large-scale energy, water and carbon balances [7].

Increasing large-scale evapotranspiration rates because of the sugarcane crop expansion has been reported [8]. Ethanol production can also affect the water quality [9]. Under these dynamic situations, the use of tools for quantifying actual evapotranspiration (ET) and biomass production (BIO) on a large scale is relevant for supporting policy plannings and decision makings about the water resources.

In Brazil, sugarcane ET has been determined by point measurements. Silva et al. [10] used the Bowen method system inside a commercial irrigated farm in a semi-arid region. Cabral et al. [11], in the São Paulo state, carried out eddy covariance measurements under rainfed conditions. However, these point studies provide specific site values and are not suitable for water productivity (WP) large-scale analyses.

BIO is a key indicator for any ecosystem [12], and its values are highly variable in both space and time. In water-limited environments, the challenge is the BIO improvements through optimized management practices [13] [14] [15] [16]. De Silva and De Costa [13] measured BIO in irrigated and rainfed sugarcane, reporting higher values

under irrigation conditions. BIO field measurements were realized under under rainfed conditions by Cabral et al. [17] in the Southern Brazil.

The difficulties of measuring and analyzing the large-scale energy, carbon and water balances with only with field measurements highlighted the importance of coupling remote sensing and weather data. These tools have been successfully used in energy crops under different climatic conditions [2] [14] [16] [18] [19].

The SAFER (Simple Algorithm for Evapotranspiration Retrieving) algorithm is applied in the current research to estimate ET on large-scale. It was developed and validated in Brazil based on simultaneous field data from four flux towers and Landsat images under strongly thermohydrological contrasting conditions [20] [21].

For large-scale BIO quantification, the radiation use efficiency (RUE) concept proposed by Monteith [22], based on the solar radiation interception, is used with satellite data. Although uncertainties arising in connection with RUE values in sugarcane crop, due to their spatiotemporal variations [23], moisture conditions [13] and cultivars [24], the model accuracy has been considered acceptable for large-scale applications with satellite data.

In France, field measurements were coupled with high-resolution FORMOSAT satellite images in irrigated maize and rainfed sunflower, where the authors attributed the main spatial BIO differences to precipitation conditions during the second crop [18]. BIO was estimated from MODIS images in Guandong, China, to evaluate the feasibility of setting up new biomass power plants and to optimize the locations of plants [25]. In Brazil, large-scale BIO estimations were done with MODIS images in maize [26] and Landsat images in sugarcane crop [27].

Despite these previous studies on energy crops, research is needed to further evaluate the combined ET and BIO models in sugarcane ecosystems, especially for operational monitoring. With a cropland mask, the SAFER algorithm to obtain ET and the RUE Monteith's model to estimate BIO are used in the sugarcane growing regions inside the São Paulo state, Brazil. Soil moisture indicators and WP in terms of the ratio of BIO to ET are analyzed by using MODIS images and weather data. The results may subsidize policies for a rational sugarcane water management. This is a very important issue under the actual scenario of water competitions with other sectors in the Brazilian Southeast, as consequences of both climate and land use changes.

Material and Methods

Study Region and Data Set

Fig. 1 shows the location of the sugarcane-growing regions, cropland mask and the weather stations in the São Paulo state, Brazil.

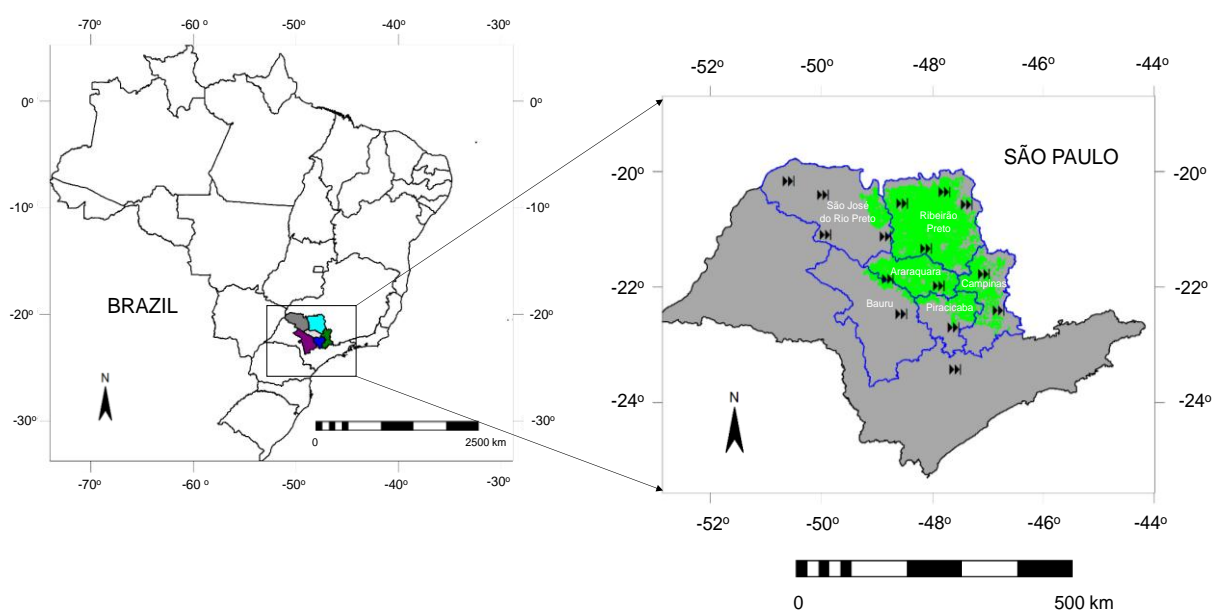


FIG. 1 LOCATION OF THE SUGAR CANE- GROWING REGIONS, THE CROP LAND MASK (GREEN AREA), AND THE WEATHER STATIONS (BLACK ARROWS)

The sugarcane-growing regions, present two well-defined seasons, one rainy and hotter and the other one dry and colder. According to Cabral et al. [17], the long-term maximum precipitation occurs in December ($274 \pm 97 \text{ mm month}^{-1}$) and the minimum one is between July and August ($27 \pm 34 \text{ mm month}^{-1}$); the annual value is $1517 \pm 274 \text{ mm yr}^{-1}$. The mean air temperatures in January and July are respectively 24°C and 19°C ; the annual average is 22°C .

MODIS images during the generalized sugarcane growing cycle (GC) from September 2011 to October 2012, inside the cropland mask, were used, along with the 15 agrometeorological stations from the National Meteorological Institute – INMET. Global solar radiation (R_G), air temperature (T_a), relative humidity (RH) and wind speed (u) were taken to calculate the reference evapotranspiration (ET_0) by the Penman-Monteith method [28]. R_G , T_a and ET_0 were averaged for over the 16-day composing periods from the MODIS MOD13Q1 reflectance products (spatial resolution of 250m) and interpolated by using the moving average method creating grids with the same spatial resolution as that for the satellite images.

This weather upscaling process was done to have representative grids of the average conditions for the same time-scale of the MODIS satellite composing images. Similar process was done by Cleugh et al. [29], who used the Penman-Monteith equation to monitor large-scale ET in Australia.

The surface temperature (T_s) product was not used because with a lower spatial resolution (1km), there was too much cloud contamination along the year in the cropland mask. Instead, T_s was retrieved by residue in the radiation balance. In addition, Cleugh et al. [29] pointed out that the use of instantaneous measurements of the radiometric T_s to calculate time-averaged fluxes lead to errors. They emphasized uncertainties in models which use the MODIS 8-day products that is a composite of once-daily overpass at $\sim 10:30 \text{ h}$ local time.

Modelling Steps

Fig. 2 shows the flowchart of the steps for modeling sugarcane water productivity components throughout SAFER and RUE applications to MODIS images without the thermal bands.

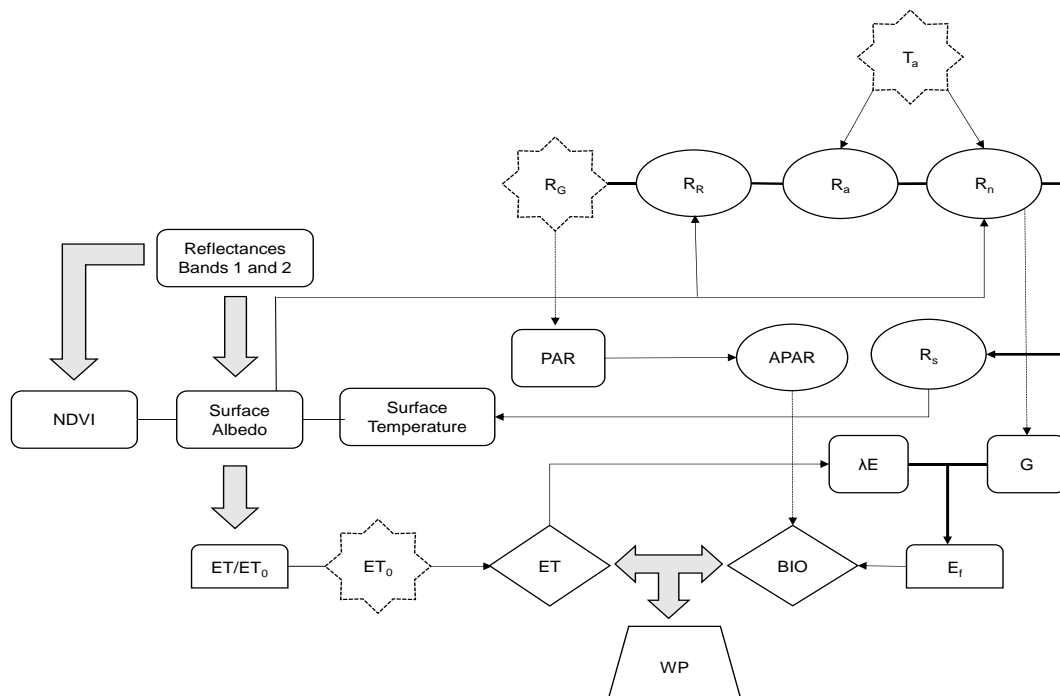


FIG. 2 FLOW-CHART FOR THE SUGARCANE WATER PRODUCTIVITY

SAFER model was elaborated and validated in Brazil with Landsat images [21], when it was called PM2. Later it was also calibrated and validated with MODIS images in the same original modelling region [15]. Field data for these validations involved irrigated crops and natural vegetation (*Caatinga*) from 2001 to 2007, being described in details in Teixeira et al. [20].

Accordingly to Fig. 2, the reflectances for the bands 1 (α_1) and 2 (α_2) were extracted from the MOD13Q1 product. This product provided cloud-free temporal composed images, at 16-day periods, throughout the generalized sugarcane GC from September 2011 to October 2012.

For the surface albedo (α_0) calculation, the following equation was applied [30]:

$$\alpha_0 = a + b\alpha_1 + c\alpha_2 \quad (1)$$

where a , b and c are regression coefficients, considered as 0.08, 0.41, 0.14, obtained under different Brazilian vegetation types and thermohydrological conditions [15].

The Normalized Difference Vegetation Index (NDVI) is an indicator related to the land cover and moisture conditions obtained from the MODIS images as follows:

$$NDVI = \frac{\alpha_2 - \alpha_1}{\alpha_2 + \alpha_1} \quad (2)$$

where α_2 and α_1 represent the reflectances over the ranges of wavelengths in the near infrared (NIR) and red (RED) regions of the solar spectrum, respectively.

R_n was estimated through the Slob equation [16] [26]:

$$R_n = (1 - \alpha_0)R_G - a_L \tau \quad (3)$$

where the regression coefficient a_L was spatially distributed through its relationship with T_a [20]:

$$a_L = dT_a - e \quad (4)$$

with d and e being the regression coefficients 6.99 and 39.93. A constant value $a_L = 110$ was applied by Bastiaanssen et al. [31] without considering thermal spatial differences.

The large-scale reflected solar radiation (R_R) was calculated as the product of R_G by α_0 [16]:

$$R_R = \alpha_0 R_G \quad (5)$$

The long-wave atmospheric radiation (R_a) was obtained by applying the Stefan-Boltzmann law:

$$R_a = \sigma \varepsilon_a T_a^4 \quad (6)$$

where σ is the Stefan-Boltzmann constant ($5.67 \times 10^{-8} \text{ W m}^{-2} \text{ K}^{-4}$) and the atmospheric emissivity (ε_a) was calculated as follows:

$$\varepsilon_a = a_a (-\ln \tau)^{b_a} \quad (7)$$

and τ is the short-wave atmospheric transmissivity calculated by the ratio of R_G to the incident solar radiation at the top of the atmosphere; a_a and b_a are the regression coefficients 0.94 and 0.10, respectively [16].

The regression coefficients of Eq. 7 are in between those obtained for Idaho ($a_a = 0.85$ and $b_a = 0.09$; [32]) and for Egypt ($a_a = 1.08$ and $b_a = 0.26$; [31]). However, even with these small differences under contrasting environmental conditions, estimate errors for these emissivities in the Brazilian sugarcane ecosystem are self-compensating when accounting for the upward and downward radiation balance components.

The surface emitted long-wave radiation (R_s) was acquired as residue in the radiation balance equation:

$$R_s = R_G - R_R + R_a - R_n \quad (8)$$

and T_s retrieved [16] [19]:

$$T_s = \sqrt[4]{\frac{R_s}{\varepsilon_s \sigma}} \quad (9)$$

The surface emissivity (ϵ_s) was calculated as follows ([16] [19]):

$$\epsilon_s = a_s \ln NDVI + b_s \quad (10)$$

where a_s and b_s are regression coefficients 0.06 and 1.00, respectively.

The original coefficients of Eq. 10 are $a_s = 0.047$ and $b_s = 1.009$ [31], being slightly different from those for Brazil. However, even with these small differences under contrasting environmental conditions, estimate errors for these emissivities in São Paulo, Brazil, are also self-cancelled in the accounting of the upward and downward radiation balance components.

With the SAFER algorithm, the ratio of actual (ET) to the reference (ET_0) evapotranspiration (ET_r) was modelled at the satellite overpass time [21]:

$$ET_r = \left\{ \exp \left[a_{sf} + b_{sf} \left(\frac{T_s}{\alpha_0 NDVI} \right) \right] \right\} \frac{ET_{0-GC}}{5} \quad (11)$$

where a_{sf} and b_{sf} are the regression coefficients 1.8 and -0.008, respectively. The correction factor ($ET_{0-GC}/5$) was applied for atmospheric demand calibration, being ET_{0-GC} the daily ET_0 grid for the sugarcane GC, and 5 mm d^{-1} is the ET_0 daily average for the same period during the original modeling conditions [19].

The daily grids of ET_0 from the agrometeorological station (black arrows in Fig. 1) were multiplied by the images resulted from Eq. 11, giving the large-scale daily ET pixel values [16] [19] [21]:

$$ET = ET_r ET_0 \quad (12)$$

For the soil heat flux (G), the equation derived by Teixeira [21] was applied:

$$\frac{G}{R_n} = a_G \exp(b_G \alpha_0) \quad (13)$$

A climatic moisture indicator for the sugarcane conditions was also considered [19]:

$$WI = P / ET \quad (14)$$

Eq. 14 enables the characterization of the climatic water component to take into account the input and output of natural water from and to the crop, indicating the potential moisture availability to the sugarcane root zones.

BIO was quantified as:

$$BIO = \epsilon_{max} E_f APAR \cdot 0.864 \quad (15)$$

where ϵ_{max} is the maximum light use efficiency, which considered the average value of 2.14 g MJ^{-1} for sugarcane [24], APAR is the fraction of absorbed photosynthetically active radiation, and 0.864 is a conversion factor [15].

APAR can be directly approximated from the Photosynthetically Active radiation (PAR), which in turn was considered as a fraction of R_G [15] [33]:

$$APAR = f_{PAR} PAR \quad (16)$$

The factor f_{PAR} was estimated from the NDVI values:

$$f_{PAR} = a_p NDVI + b_p \quad (17)$$

where the coefficients a_p and b_p of 1.257 and -0.161, respectively, reported for a mixture of arable crop types [33] were considered.

The water productivity (WP) based on evapotranspiration [15] [26] was considered as:

$$WP = BIO / ET \quad (18)$$

Results and Discussion

Weather Conditions and Sugarcane Phases

Fig. 3 presents the trends for the totals of precipitation (P) and ET_0 together with that for the R_G daily averages.

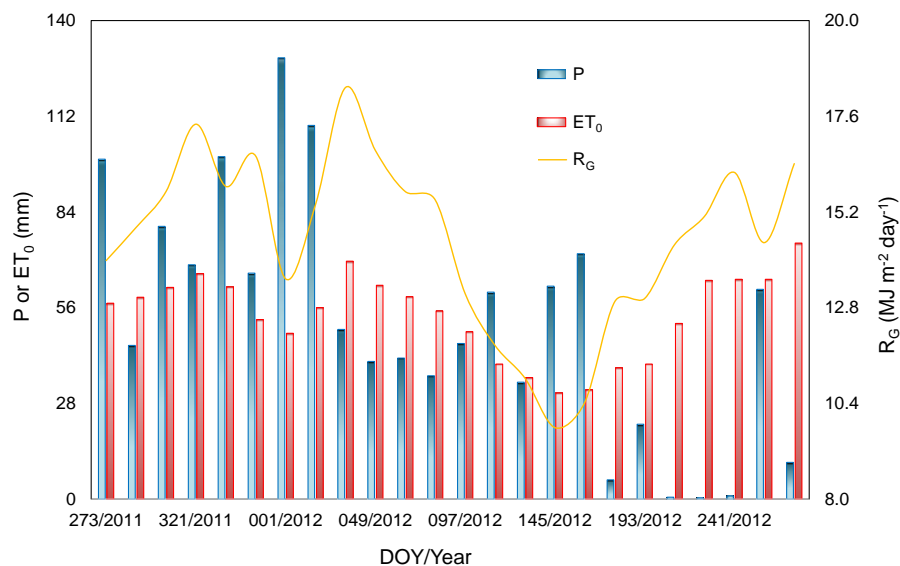


FIG. 3 SEASONAL VARIATIONS OF THE AVERAGE VALUES FOR GLOBAL SOLAR RADIATION (R_G); AND TOTALS OF PRECIPITATION (P) AND REFERENCE EVAPOTRANSPIRATION (ET_0)

The values depicted in Fig. 3 are for each the MODIS 16-day periods, inside the generalized sugarcane GC, in the growing regions of the São Paulo state, Brazil. The weather data resulted from the interpolation processes in the cropland mask, from September 2011 to October 2012 in terms of Day of the Year (DOY)

Following Silva et al. [10], the sugarcane phases may be divided into four: Phase 1 – Germination and Establishment; Phase 2 – Tillering; Phase 3 – Grand Growth; and Phase 4 – Ripening and Maturation.

Phase 1 denotes activation and subsequent sprouting of the vegetative bud. It is influenced by soil moisture, soil temperature and soil aeration. Phase 2 starts from around 40 days after the GC initiation and may last up to 120 days. Variety, R_G , T_a , soil moisture and fertilization influence this phase. Phase 3 starts from 120 days after the GC starting and lasting up to 270 days in a 12-month crop. High both, soil moisture and R_G levels, favor better cane elongation during this phase. Phase 4 in a 12-month sugarcane crop lasts for about three months starting from 270-360 days after the GC initiation. High R_G levels and low soil moisture conditions are favorable during this phase. This last phase is characterized by slower growth activity [34].

From Fig. 3, the highest values of both R_G and ET_0 , were observed between the Phases 2 and 3, from November (DOY 321/2011) to early April (DOY 097/2012). In that period, mean R_G reached to rates above $20\ MJ\ m^{-2}\ day^{-1}$, promoting ET_0 over $4.5\ mm\ day^{-1}$, being favorable for BIO.

Rainfalls of 1240 mm in total for the entire generalized GC, although being below the long-term value of the study area, were well distributed along the crop phases. Cabral et al. [17] reported a 13% of BIO reduction in relation to the regional average in São Paulo state, Brazil, as a consequence of the lower natural water availability observed during the initial 120 days of cane re-growth. However, in the current research, a short drier period was verified from late June to the second half of August (DOY 177 to 257 of 2012), corresponding to periods inside Phase 3, which should have caused some crop water deficit, when sugarcane water requirements are high.

For rainfed sugarcane crop, a GC precipitation between 1100 and 1500 mm with good distribution is considered adequate. During the active growth phases, water deficit could reduce the leaf area, affecting the number of tillers and leaves per stalk [35]. However, during Phase 4, rains are not desirable because they lead to poor juice quality [34]. The decline in rainfall at the end of the GC was then favorable for sugarcane WP.

Actual Evapotranspiration

Fig. 4 shows the spatial distribution of the sugarcane ET daily averages, for the 16-day period MODIS images, from September 2011 to October 2012 in the growing areas of the São Paulo state, Brazil.

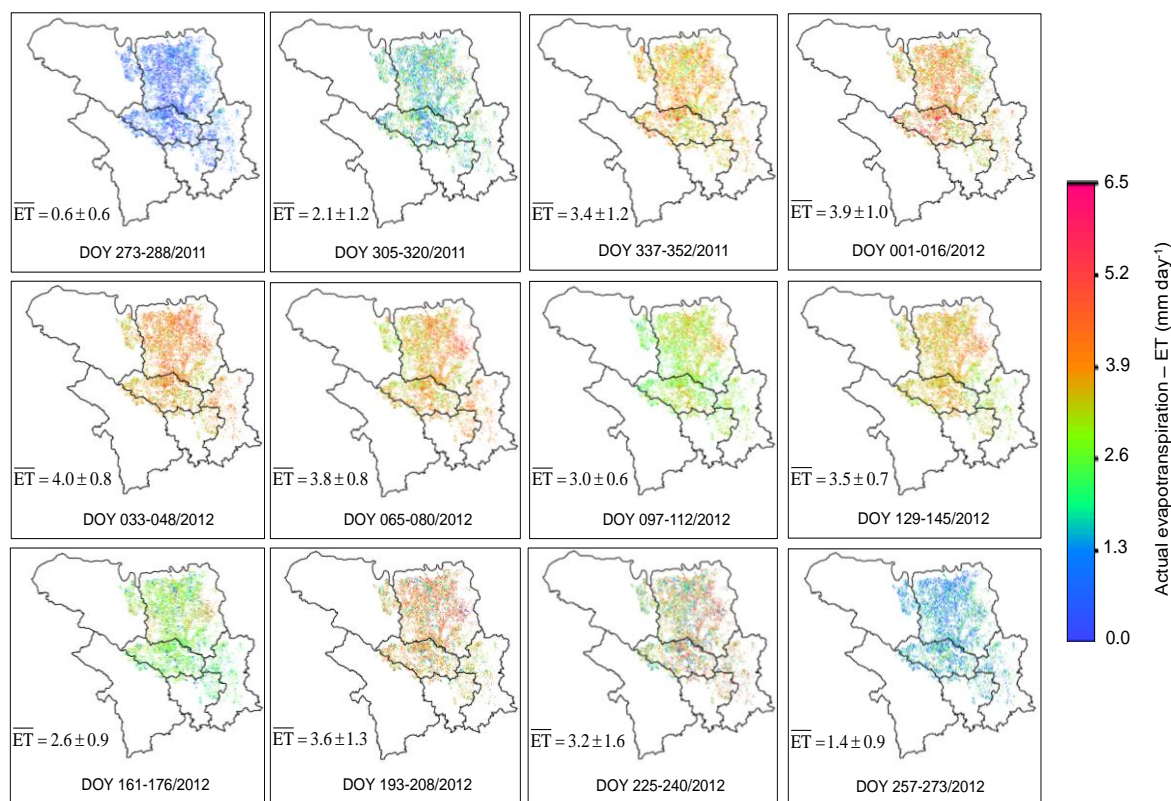


FIG. 4 SPATIAL DISTRIBUTION FOR THE 16-DAY AVERAGE VALUES OF THE SUGARCANE EVAPOTRANSPIRATION (ET)

The spatial and temporal ET variations are evident inside the cropland mask, along the generalized rainfed sugarcane GC from September 2011 to October 2012. The strong contrast is noticed mainly when looking for the pixels in the images of DOY 273-288/2011 and 033-048/2012. The maximum values were verified under high both rainfall amount and atmospheric demand (see Fig. 3 and 4), in early February 2012, when the daily average for ET was 4.0 mm day⁻¹ (DOY 033-048/2012), inside the Phase 3. The lowest ET rates, below 1.5 mm day⁻¹, took place in the Phase 1, from DOY 273 to 305 of 2011 and at the end of Phase 4, from the second half of September (DOY 257/2012) to the first half of October (DOY 281/2012).

In relation to the ET spatial variations, the lowest standard deviation (SD) values (0.6 mm day⁻¹) happened also at the start of the generalized GC (Phase 1), while the highest ones (1.6 mm day⁻¹) were in Phase 4, at the end of the rainy season (see Figs. 3 and 4).

In the mixture of sugarcane plants, inside the cropland mask, average ET ranged from 0.6 to 4.0 mm day⁻¹, with a mean GC value of 3.0 mm day⁻¹. The total ET for a GC of 400 days was 1180 mm. The ET daily values were above those reported by Eksteen et al. [36], who found rates between 1.6 and 2.9 mm day⁻¹, involving different sugarcane varieties and soil moisture conditions. However, a previous study with sugarcane, under irrigation conditions, in Everglades, Florida (USA), by Omary and Izuno [37], resulted in minimum daily rates of 0.7 to 1.5 mm day⁻¹, and maximums of 4.5 to 4.6 mm day⁻¹, with a total GC of 1060 mm. The similar values of the current study with that one in Florida provide confidence for the application of the SAFER algorithm to MODIS images and without the thermal band.

Soil Moisture Indicators

Fig. 5 shows the ET_r and WI average trends, throughout the generalized sugarcane GC, in the growing regions of the São Paulo state, Brazil, in terms of Day of the Year (DOY).

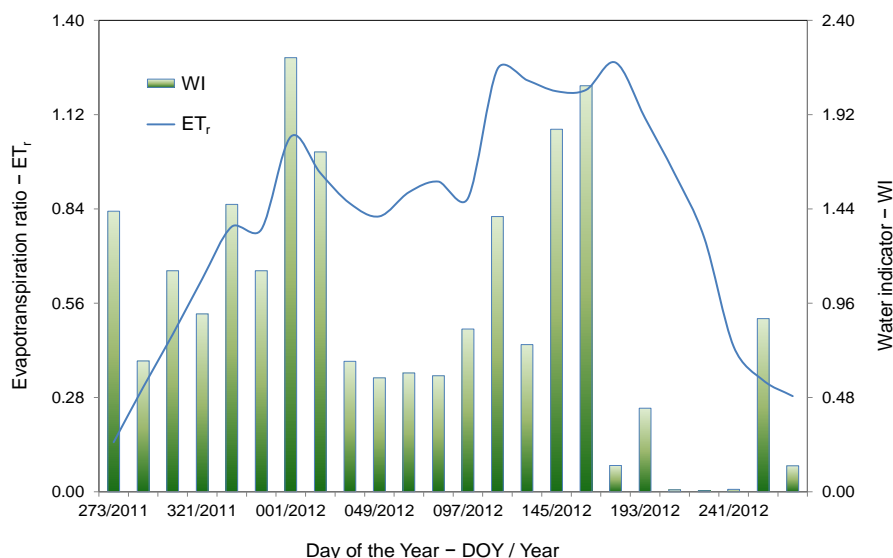


FIG. 5 SOIL MOISTURE INDICATORS. ET_r : RATIO OF ACTUAL (ET) TO REFERENCE (ET_0) EVAPOTRANSPIRATION; WI : RATIO OF PRECIPITATION (P) TO ET

Declines in ET_r values occurred between DOY 017 and 113 of 2012, inside the Phase 3, but not dropping below 0.80. The maximums, above 1.20 at the end of this phase, were observed from the middle April to the middle May in the year 2012. ET_r in rainfed crops can be used to characterize the moisture status in the root zones [38], while under good irrigation conditions it is considered as the crop coefficient (K_c), being used for irrigation management [28] [39].

Sugarcane K_c values, fully covering the soil, were reported to be between 1.1 and 1.5, depending on the weather conditions [36], being typically around 1.25 [28] [39] as it was verified in the Phase 3 of the current study. These similarities again bring confidence for the SAFER application to MODIS images. Although the ET_r curve pictured in Fig. 5 being for rainfed sugarcane crop, the maximum values corresponded to K_c under optimum irrigation conditions, except for the period between DOY 017 to 113 in the year 2012.

Throughout the trend of the WI indicator, one can see that its values followed those for ET_r . However, the decline on ET_r was not as deep as it was on WI during Phase 3. This fact means that even with P reduction during this phase, the soil moisture still kept the rainfed sugarcane development. In average, the ET rates accounted for 80% of those for the reference grass ($K_c = 0.80$); and rainfalls, in general, met the crop water requirements satisfactorily, with P representing 90% of ET ($WI = 0.90$). However, supplementary irrigation should be economically feasible during Phase 3, wherever there is water available for this practice, especially by using efficient methods such as drip irrigation, which could improve the sugarcane WP.

Biomass Production

Fig. 6 shows the spatial distribution of the sugarcane BIO daily averages, for the 16-day period MODIS images, from September 2011 to October 2012, in the growing areas of the São Paulo state, Brazil.

As there is a relationship between ET and BIO [15], the periods with the highest BIO are the same as those for ET , inside the Phase 3, with BIO pixel values above $200 \text{ kg ha}^{-1} \text{ day}^{-1}$. The lowest ones took place at the start of the Phase 1, from DOY 273 to 305 of 2011, and at the end of the Phase 4, from DOY 257 to 281 of 2012, when they were below $50 \text{ kg ha}^{-1} \text{ day}^{-1}$.

Rainfall, in general, favored BIO, providing good moisture levels in the root zone of the sugarcane crop, in the whole generalized GC, except at the end of Phase 4, when low rain amounts are favorable for juice quality for the rainfed canes. The short period of lowering P , during Phase 3, even with an increased atmospheric demand - as observed by the ET_0 values, did not significantly reduced BIO (see Figs. 3 and 6). However, as in the case of ET , a decline in the BIO values was observed at the transition of Phase 3 to Phase 4, what is considered common to

happen in sugarcane crop [23].

Although high R_G levels increasing the atmospheric demand, i.e high ET_0 values, in Phase 4, the low rainfall amounts did not contribute to raise BIO values (see Figs. 3 and 5).

The variation of the BIO SD values followed those for ET, with the lowest ($22 \text{ kg ha}^{-1} \text{ day}^{-1}$) and the highest ($88 \text{ kg ha}^{-1} \text{ day}^{-1}$) in the Phases 1 and 4, respectively.

Under irrigation conditions, Oliver and Singels [40] reported strong BIO declines, when water application was reduced by 50%, depending on the sugarcane variety. However, Andrade et al. [27] affirmed that the soil moisture effects on BIO vary also according to the planting and harvesting dates. In South Africa, Donaldson et al. [24] reported seasonal variations affecting BIO in a number of sugarcane cultivars, being the ranges between 90 and $184 \text{ kg ha}^{-1} \text{ day}^{-1}$.

In a study with irrigated sugarcane crop, in the Minas Gerais, Brazil, Andrade et al. [27] obtained average BIO values within the range between 100 and $160 \text{ kg ha}^{-1} \text{ day}^{-1}$, similar to those from our study, during several crop periods. BIO increases can be reached by improvements on the natural resources use, mainly throughout R_G interception and water management [36].

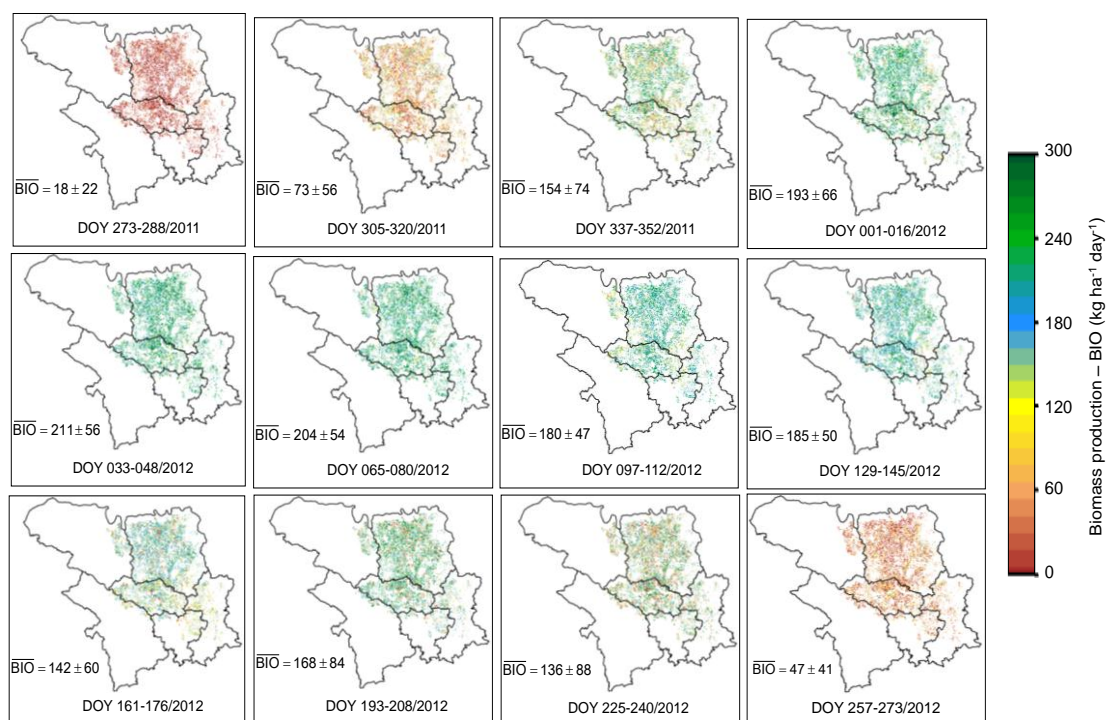


FIG. 6 SPATIAL DISTRIBUTION FOR THE 16-DAY AVERAGE VALUES OF THE SUGARCANE BIOMASS PRODUCTION (BIO)

Water Productivity

Fig. 7 shows the pixel averages and standard deviations (SD) of the sugarcane WP, for the 16-day period MODIS images, and a generalized GC from September 2011 to October 2012 in the growing areas of the São Paulo state, Brazil.

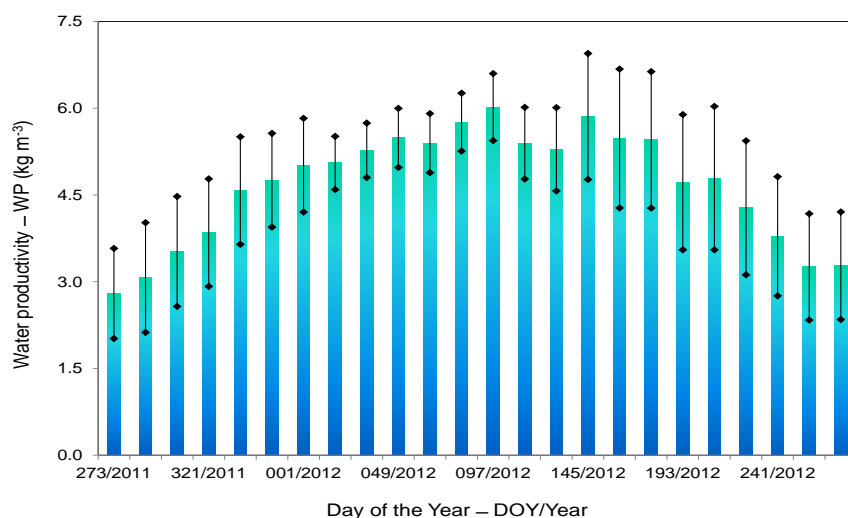
Sugarcane WP values started with an average of 2.5 kg m^{-3} in Phase 1. They increased to around 4.4 kg m^{-3} during Phase 2, going to a mean value of 5.4 kg m^{-3} in Phase 3 to fall again to an average of 3.7 kg m^{-3} in Phase 4. For the entire generalized GC, the mean value was 4.4 kg m^{-3} . The short rainfall reductions during Phase 3 did not drop WP values below 4.5 kg m^{-3} . The lowest SD happened during the rainy period, at the start of the Phase 3, while the highest ones were toward the end of this phase to the start of Phase 4.

Cabral et al. [17], through eddy covariance measurements found similar sugarcane WP for two growing cycles in the São Paulo state, Brazil, averaging 4.2 kg m^{-3} . Chooyok et al. [5] reported sugarcane WP of 5.8 and 6.5 kg m^{-3} for two distinct regions of Thailand, concluding that these values depend on climate, soil, and planting date. Eksteen

et al. [36] in South Africa found WP values between 5.8 and 7.8 kg m⁻³ for different sugarcane varieties and irrigation regimes. However, according to Chooyok et al. [5], the global sugarcane WP average is around 4.8 kg m⁻³, matching well with the mean pixel values of our study, when considering the generalized GC. These agreements provide confidence to the models used for ET and BIO with MODIS images and without the thermal band, in the sugarcane growing areas of São Paulo state, Brazil.

Considering the importance of sugarcane crop, for sugar and alcohol production, and also for generating renewable energy, the high WP values under rainfed conditions, with sustainable crop management, can compensate the negative effects of land use changes caused by its fast expansion in the Southeast Brazil.

The monitoring of the sugarcane WP dynamics on large scale in the main growing regions of Brazil is very important because of the actual scenario of water competitions with other sectors, as consequences of both climate and land use changes.



REFERENCES

- [1] Mello, C.O., and Esperancini M.S.T. "Análise econômica da eficiência da produção de cana-de-açúcar de fornecedores do Estado do Paraná." *Revista Energia na Agricultura* 27 (2012): 48–60.
- [2] Rudorf, B.F.T., et al. "Studies on the rapid expansion of sugarcane for ethanol production in São Paulo State (Brazil) using Landsat Data." *Remote Sensing* 2 (2010): 1057–1076.
- [3] Scharlemann, J.P., and Laurance, W.F. "How Green Are Biofuels?" *Science* 319 (2008): 43–44.
- [4] Waclawovsky, A.J., Sato, P.M., Lembke, C.G., Moore, P.H., and Souza, G.M. "Sugarcane for bioenergy production: an assessment of yield and regulation of sucrose content." *Plant Biotechnology Journal* 8 (2010): 1–14.
- [5] Chooyok, P., Pumijumnog, N., and Ussawarujikulchai, A.T. "The water footprint assessment of ethanol production from molasses in Kanchanaburi and Supanburi province of Thailand." *Procedia APCBEE* 5 (2013): 283–287.
- [6] Beringer, T., Lucht, W., and Schaphoff, S. "Bioenergy production potential of global biomass plantations under environmental and agricultural constraints." *GCB Bioenergy* 3 (2011): 299–312.
- [7] Cerri, C.C.; Galdos, M.V., Maia, S.M.F., Bernoux, M., Feigl, B.J., Powlson, D., and Cerri, C.E.P. "Effect of sugarcane harvesting systems on soil carbon stocks in Brazil: an examination of existing data." *European Journal of Soil Science* 62 (2011): 23–28.
- [8] Anderson-Teixeira, K.J. et al. "Climate-regulation services of natural and agricultural ecoregions of the Americas." *Nature Climate Change* 2 (2012): 177–181.
- [9] Gunkel, G. et al. "Sugar cane industry as a source of water pollution-case study on the situation in Ipojuca River, Pernambuco, Brazil." *Water, Air & Soil Pollution* 180 (2007): 261–269.
- [10] Silva, T.G.F. da et al. "Demanda hídrica e eficiência do uso da água da cana-de-açúcar irrigada no semiárido brasileiro." *Revista Brasileira de Engenharia Agrícola e Ambiental* 15 (2011): 1257–1265.
- [11] Cabral, O.M.R. et al. "Water use in a sugar-cane plantation." *GCB Bioenergy* 4 (2012): 555–565.
- [12] Wu, C., Munger, J.W., Niu, Z., and Kuanga, D. "Comparison of multiple models for estimating gross primary production using MODIS and eddy covariance data in Havard Forest." *Remote Sensing of Environment* 114 (2010), 2925–2939.
- [13] De Silva, A.L.C., and De Costa, W.A.J.M. "Growth and radiation use efficiency of sugarcane under irrigated and rain-fed conditions in Sri Lanka." *Sugar Tech* 14 (2012): 247–254.
- [14] Adak, T., Kumar, G., Chakravarty, N.V.K., Katiyar, RK, and Deshmukh, P.S. "Biomass and biomass water use efficiency in oilseed crop (*Brassica Jnceae* L.) under semi- arid microenvironments." *Biomass and Bioenergy* 51 (2013): 154–162.
- [15] Teixeira, A.H. de C.; Scherer-Warren, M.; Hernandez, F.B.T.; Andrade, R.G., and Leivas, J.F. "Large-Scale Water Productivity Assessments with MODIS Images in a Changing Semi-Arid Environment: A Brazilian Case Study." *Remote Sensing* 11 (2013): 5783–5804.
- [16] Teixeira, A.H. de C., Hernandez, F.B.T., Lopes, H.L., Scherer-Warren, M., and Bassoi, L.H. "A Comparative Study of Techniques for Modeling the Spatiotemporal Distribution of Heat and Moisture Fluxes in Different Agroecosystems in Brazil." In *Remote Sensing of Energy Fluxes and Soil Moisture Content*, edited by George P. Petropoulos, 169-191. CRC Group, Taylor and Francis, Boca Raton, Florida, 2014.
- [17] Cabral, O.M.R. et al. "Fluxes of CO₂ above a sugarcane plantation in Brazil." *Agricultural and Forest Meteorology* 182-183 (2013): 54–56.
- [18] Claverie, M. et al. "Maize and sunflower biomass estimation in southwest France using spatial and temporal resolution remote sensing data." *Remote Sensing of Environment* 124 (2012), 884–857.
- [19] Teixeira, A.H. de C. et al. "Water balance indicators from MODIS images and agrometeorological data in Minas Gerais state, Brazil." *Proceedings of SPIE* 9637 (2015), 963700-1–14.
- [20] Teixeira, A.H. de C., Bastiaanssen, W.G.M., Ahmad, M–ud–D, Bos, M.G., and Moura, M.S.B. "Analysis of energy fluxes and vegetation-atmosphere parameters in irrigated and natural ecosystems of semi-arid Brazil." *Journal of Hydrology* 362 (2008): 110–127.

- [21] Teixeira A.H. de C. "Determining regional actual evapotranspiration of irrigated and natural vegetation in the São Francisco river basin (Brazil) using remote sensing and Penman-Monteith equation." *Remote Sensing* 2 (2010): 1287–1319.
- [22] Monteith, J.L. "Solar radiation and productivity in tropical ecosystems." *Journal of Applied Ecology* 9 (1972): 747–766.
- [23] van Heerden, P.D.R., Donaldson, R.A., Watt, D.A., and Singels, A. "Biomass accumulation in sugarcane: unravelling the factors underpinning reduced growth phenomena." *Journal of Experimental Botany* 61 (2010): 2877–2887.
- [24] Donaldson, R.A., Redshaw, K.A., Rhodes, R., and van Anterpen, R. "Season effects on productivity of some commercial South African sugarcane cultivars, I: Biomass and radiation use efficiency." *Proceedings of the South Africa Sugar Technology Association* 81 (2008): 517–527.
- [25] Shi, X. et al. "Using spatial information technologies to select sites for biomass power plants: A case study in Guangdong, China." *Biomass and Bioenergy* 32 (2008): 35–43.
- [26] Teixeira, A. H. de C. et al. Coupling MODIS images and agrometeorological data for agricultural water productivity analyses in the Mato Grosso state, Brazil. *Proceedings of SPIE* 9239 (2014): 92390W-1-92390W-14.
- [27] Andrade, R.G., Sediya, G., Soares, V.P., Gleriani, R.G., and Menezes, S.J.M.C. "Estimativa da produtividade da cana-de-açúcar utilizando o SEBAL e imagens Landsat." *Revista Brasileira de Meteorologia* 29 (2014): 433–442.
- [28] Allen, R.G., Pereira, L.S., Raes, D., and Smith, M.. "Crop evapotranspiration. Guidelines for computing crop water requirements." *FAO Irrigation and Drainage Paper* 56, Rome, Italy, 300 pp, 1998.
- [29] Cleugh, H.A., Leuning, R., Mu, Q., and Running, S.W. "Regional evaporation estimates from flux tower and MODIS satellite data." *Remote Sensing of Environment* 106 (2007): 285–304.
- [30] Valiente, J.A., Nunez, M., Lopez-Baeza, E., and Moreno, J.F. "Narrow-band to broad-band conversion for Meteosat visible channel and broad-band albedo using both AVHRR-1 and -2 channels." *International Journal of Remote Sensing* 16 (1995): 1147–1166.
- [31] Bastiaanssen, W.G.M., Menenti, M., Feddes, R.A., Roerink, G.J., and Holtslag, A.A.M. "A remote sensing surface energy balance algorithm for land (SEBAL) 1. Formulation." *Journal of Hydrology* 212–213 (1998): 198–212.
- [32] Allen, R.G., Hartogensis, O., and de Bruin, H.A.R. "Long-wave radiation over alfalfa during the RAPID field campaign in southern Idaho." *Research Report*, Kimberly, University of Idaho, Id, 2000.
- [33] Bastiaanssen, W.G.M., and Ali, S. "A new crop yield forecasting model based on satellite measurements applied across the Indus Basin, Pakistan." *Agriculture, Ecosystems & Environment* 94 (2003): 32–340.
- [34] Tejera, N.A.; Rodes, R., Ortega, E., Campos, R., and Lluch, C. "Comparative analysis of physiological characteristics and yield components in sugarcane cultivars." *Field Crops Research* 102 (2007), 64–72.
- [35] Inman-Bamber, N.G., and Smith, D.M. "Water relations in sugarcane and response to water deficits." *Field Crops Research* 92 (2005): 185–202.
- [36] Eksteen, A., Singels, A., and Ngxaliwe, S. "Water relations of two contrasting sugarcane genotypes." *Field Crops Research* 168 (2014), 86–100.
- [37] Omary, M., and Izuno, F.T. "Evaluation of sugar-cane evapotranspiration from water table data in the everglades agricultural area." *Agricultural Water Management* 27 (1995): 309–319.
- [38] Lu, N., Chen, S., Wilske, B., Sun, G., and Chen, J. "Evapotranspiration and soil water relationships in a range of disturbed and undisturbed ecosystems in the semi-arid Inner Mongolia, China." *Journal of Plant Ecology* 4 (2011): 49–60.
- [39] Inman-Bamber, N.G., and McGlinchey, M.G. "Crop coefficients and water-use estimates for sugarcane based on long-term Bowen ratio energy balance measurements." *Field Crops Research* 83 (2003): 125–38.
- [40] Oliver, F.C., and Singels, A. "Water use efficiency of irrigated sugarcane as affected by variety and row spacing." *Proceedings of the South Africa Sugar Technologist Association* 77 (2003), 347–351.